*Macromolecules* **2004,** *37,* 501−506

# One-Step Formation of Morphologically Controlled Nanoparticles with Projection Coronas

**Tatsuo Kaneko,[†] Kazuhiro Hamada,[†] Ming Qing Chen,[‡] and Mitsuru Akashi*,[†,§]**

*Department of Nanostructured and Advanced Materials, Graduate School of Science and Engineering, Kagoshima University, 1-21-40, Korimoto, Kagoshima 890-0065, Japan; School of Chemical and Material Engineering, Southern Yangtze University, Wuxi 214036, P. R. China; and Department of Molecular Chemistry, Graduate School of Engineering, Osaka University, 2-1, Yamada-oka, Suita 565-0871, Japan and CREST, JST, 4-1-8, Hommachi, Kawaguchi, 332-0012, Japan*

*Received August 28, 2003; Revised Manuscript Received October 17, 2003*

ABSTRACT: Nanoparticles with projection coronas were prepared by the one-step dispersion terpolymerization of styrene, acrylonitrile, and poly(ethylene glycol) monomethacrylate in ethanol−water solution, and their morphologies were controlled. When the mole composition of acrylonitrile to the total monomers $C_{AN}$ was 0.49−0.66, electron microscopy showed that the nanoparticles were spherical and had a number of projections on the surface. A $C_{AN}$ of more than 0.66 yielded no nanospheres, and a $C_{AN}$ smaller than 0.49 yielded projection-free nanospheres. The morphology of the nanospheres could be controlled by changing the reaction conditions, and some conditions yielded a regular arrangement of uniform projections on the surface similar to that seen in some coronaviruses. X-ray and spectroscopic studies suggested that the projections might be formed as a result of the nonequilibrated swelling of acrylonitrile and poly(ethylene glycol) domains on the surface.

## Introduction

Nanoparticles have been widely studied because of their wide potential in the manufacture of biomedical products,[1,2] optical devices,[3] and other industrial materials.[4] Morphology control is expected to be one approach in the development of advanced materials. In inorganic systems, particles with various nonspherical morphologies have been prepared by anisotropic crystallization, i.e., self-organization on the element level.[5,6] In systems utilizing organic molecules, morphologically anisotropic microparticles in the morphology of dumbbells,[7] bowls,[8] snowmen,[9] raspberries,[10] viruses,[11,12] and so on have been prepared by multistep preparation methods such as seed polymerization[7−9] and heteroaggregation.[10−12] Selective removal of one component from particles composed of more than two components gives rise to hollow[13] and/or porous particles.[14] While multistep methods are widely used, they are very complicated. On the other hand, the one-step method is not only facile but also important in the field of the molecular organization. We have developed a one-step method for the preparation of polymeric nanoparticles with a spherical morphology from hydrophobic monomer and a hydrophilic macromonomer through self-organization.[15] The nanoparticles prepared by the radical polymerization from styrene, acrylonitrile, and poly(ethylene oxide) monomethacrylate had many projections on their surface.[16] We have already shown that manipulation of solvent composition (ethanol/water mixture) and macromonomer content relative to total monomers can be used to effectively control the size of particles, although the control of particle morphology has not yet been achieved. The control of nanoparticle morphology by a one-step synthetic procedure is important in the field of not only the nanoconstruct preparation but also the self-organization at the polymer chain level which is a base of formation of the biological nanoconstructs such as viruses and organelles.

In the present study, we attempted to control the morphology of nanoparticles and to clarify the mechanism of projection formation by changing reaction conditions such as reaction time and styrene/acrylonitrile compositions. Certain reaction conditions gave a monodispersed polymeric nanoparticle having uniform projections regularly arranged on the particle surface, with some projections showing a hexagonal arrangement like viruses.[17]

## Experimental Section

**Materials.** Styrene (St; WAKO Pure Chemical Ind. Ltd.) and acrylonitrile (AN; WAKO Pure Chemical Ind. Ltd.) which were used as monomers were distilled in vacuo just before use. Poly(ethylene glycol) monomethacrylate (PEGm; number-average molecular weight $M_n = 1740$) donated from Nippon Oil and Fats Co. was used as received. 2,2′-Azobis(isobutyronitrile) (AIBN; WAKO Pure Chemical Ind. Ltd.) which was used as a radical initiator was recrystallized from methanol before use. A mixture of distilled water and ethanol (WAKO Pure Chemical Ind. Ltd.) was used as the polymerization medium.

**Polymerization.** Dispersion polymerizations of St, AN, and PEGm were carried out batchwise in a glass tube. The general procedure used to prepare all of the nanospheres was as follows: St, AN (total amount of St and AN, 3.9 mmol), PEGm (0.027 mol), and AIBN (1 mol % of total monomers) were added to the ethanol/water (4/1 v/v, 5 mL) mixture. Each polymerization batch was prepared in a glass tube and was repeatedly degassed by freeze−thaw cycles in a vacuum apparatus, sealed off, and then placed in an incubator at 60 °C for 1−24 h. The resulting solutions were first dialyzed in distilled deionized water using a cellulose dialyzer tube to remove unreacted monomer. The latex particles were then centrifuged and redispersed in water.

---

[†] Kagoshima University.

[‡] Southern Yangtze University.

[§] CREST, JST and Osaka University.

* Correspondence author: Tel +81-99-282-8320; Fax +81-99-255-1229; e-mail akashi@chem.eng.osaka-u.ac.jp.

10.1021/ma035276g CCC: $27.50 © 2004 American Chemical Society
Published on Web 12/23/2003

**Table 1. Synthesis and Characterization of Poly(St-*co*-AN-*co*-PEGm) with Various Monomer Compositions**[a]

| run | St (mmol) | AN (mmol) | PEGm (mmol) | comp in feed (St:AN:PEGm) | comp in terpolymer[b] (St:AN) | N/C[c] | O/C[c] | yield (wt %) |
|---|---|---|---|---|---|---|---|---|
| 1 | 0.30 | 3.6 | 0.027 | 0.08:0.92:0.007 | 0.34:0.66 | 0.31 | 0.52 | 20 |
| 2 | 0.50 | 3.4 | 0.027 | 0.13:0.87:0.007 | 0.37:0.63 | 0.25 | 0.50 | 29 |
| 3 | 0.70 | 3.2 | 0.027 | 0.18:0.82:0.007 | 0.41:0.58 | 0.26 | 0.69 | 41 |
| 4 | 0.90 | 3.0 | 0.027 | 0.23:0.76:0.007 | 0.45:0.55 | 0.24 | 0.56 | 48 |
| 5 | 1.1 | 2.8 | 0.027 | 0.28:0.71:0.007 | 0.47:0.52 | 0.22 | 0.52 | 52 |
| 6 | 1.3 | 2.6 | 0.027 | 0.33:0.66:0.007 | 0.51:0.49 | 0.15 | 0.69 | 53 |

[a] St, AN, and PEGm refer to styrene, acrylonitrile, and poly(ethylene glycol) monomethacrylate, respectively. Reaction time was 24 h; temperature was 60 °C; solvent was a mixture of water and ethanol (water/ethanol = 1v/4v); $M_n$ of PEGm is 1740. [b] Determined by $^1$H NMR spectra. [c] N/C and O/C refer to the molar ratio of nitrogen to carbon and that of oxygen to carbon, respectively, which were determined by ESCA.

**Measurements.** $^1$H NMR spectra of the terpolymers were measured using two solvents, chloroform-*d* and dimethyl-$d_6$ sulfoxide, with a NMR spectrometer (JEOL FX 400) at 400 MHz. $^1$H NMR chemical shifts in parts per million (ppm) were recorded downfield from 0.00 ppm using tetramethylsilane (TMS) as an internal reference.

Fourier transformation infrared (FT-IR) spectra of the particle surface were recorded by the attenuated total reflection (ATR) method on a Perkin-Elmer Spectrum One FT-IR spectrometer after 64 scans (4 cm$^{-1}$ resolution) over the range from 4600 to 600 cm$^{-1}$.

The molecular weight of the polymers was determined by gel permeation chromatography (GPC; Shimadzu LC-6A system with a TSK-GEL Super H2000 column) calibrated with poly(ethylene oxide) standards (eluent: dimethylformamide).

X-ray diffraction patterns were taken with a Geigerflex RAD-II B (RIGAKU) emitting Ni-filtered Cu K$\alpha$ radiation (30 kV, 15 mA) at scanning angles ranging from 30° to 6° at a scanning rate of 2° min$^{-1}$.

Electron spectroscopy for chemical analysis (ESCA) was performed with a Shimadzu ESCA 1000 apparatus employing Mg K$\alpha$ radiation (1253.6 eV) and a pass energy of 31.5 eV. The higher resolution utility scans were used to determine the atomic concentrations of carbon, nitrogen, and oxygen.

The surface of the nanospheres was observed on a stage for scanning electron microscopic (SEM) observation with a HITACHI S-4100H SEM, after gold was spattered onto the samples at a thickness of approximately 20 nm.

Transmission electron microscopy (TEM) images were obtained with a Hitachi H-700H microscopic operated at an acceleration voltage of 150 kV at a magnification of 100 000×. Specimens were prepared by slow evaporation of a drop of approximately diluted solution deposited onto a collodion-coated copper mesh grid followed by carbon spattering.

## Results and Discussion

**Effects of Styrene/Acrylonitrile Composition.** Spherical nanoparticles with a number of projections were prepared by the terpolymerization of St, AN, and PEGm in a mixed solvent comprised of ethanol/water (4/1 v/v) at 60 °C for 24 h in vacuo as shown in the previous paper.[16] On the other hand, the copolymerization of St and PEGm gave projection-free nanospheres with an St core and PEGm corona.[18] These facts suggest that AN plays an important role in the projection's formation. The poly(St-*co*-AN-*co*-PEGm)s were then prepared using various molar compositions of AN to total monomers in feed, $c_{AN} = 0.66$, 0.72, 0.77, 0.82, 0.87, 0.92, and 1.00, and the particle formation behaviors were investigated. The FT-IR/ATR spectra of the purified polymers showed the distinct absorption spectra representing the vibration of cyano groups (2239 cm$^{-1}$), aromatic rings (3028, 1602, 761 cm$^{-1}$), ether groups (1098 cm$^{-1}$), and alkylene groups (1494, 1453, 2925 cm$^{-1}$), confirming that these samples were composed of all of the monomeric units. Using the $^1$H NMR spectra, we estimated the St and AN composition of the polymers from the integration values of the PEGm methylene peak at a chemical shift of 3.6 ppm, the aromatic proton peaks of St in the region of 6.5−7.4 ppm, and the whole proton peaks of main chains in the region of 0.8−3.3 ppm. The results are summarized in Table 1. Since the composition of PEGm units was too low to be estimated by $^1$H NMR study, it was assumed to be equal to the composition in the feed. One can see that the composition of AN to the total monomers in the terpolymers, $C_{AN}$, was lower than in the feed. These results suggest that the AN monomer was less reactive than St, which corresponds to the reactivity ratios of St and AN in emulsion polymerization systems, $r_1 = 0.52$ and $r_2 = 0.03$ ($M_1$:St and $M_2$:AN), as reported in the literature.[19] St and methyl methacrylate (MMA) show little difference in the reactivity ratios, $r_1 = 0.52$ and $r_2 = 0.46$ ($M_1$: St and $M_2$: MMA), according to the literature.[20] We can guess that PEGm has a reactivity similar to that of MMA and then with St in terms of the electronic environment of the double bond. PEGm should also be less reactive than St in the present system because of the very low concentration of PEGm in the feed. As a consequence, St may be polymerized preferentially to AN and PEGm. Yields of the polymers were 20−53%. Number-average molecular weight, $M_n$, and weight-average molecular weight, $M_w$, of terpolymers were $9.0 \times 10^3 - 2.5 \times 10^4$ and $5.2 \times 10^4 - 1.6 \times 10^5$, respectively, and increased with St composition, which may be attributed to the highest reactivity of St. The resulting nanospheres showed a wide molecular weight distribution, $M_w/M_n$, in the range 6.1−7.2, which may be attributed to the difference in reactivity and molecular weight of the monomers. We speculate that St may react preferentially at the early stage of the polymerization to give St-rich chains with a larger $M_n$ while AN may react subsequently to give AN-rich chains with a smaller $M_n$.

The water-dispersed terpolymers with various $C_{AN}$ were observed by TEM. When $C_{AN}$ was 0.49 ($c_{AN} = 0.66$), spherical particles with a diameter of about 350 nm were formed, and many projections were present on the surfaces (Figure 1A). When $C_{AN}$ increased to 0.52 ($c_{AN} = 0.71$) and 0.55 ($c_{AN} = 0.76$), the nanosphere showed a decrease in size, but the projections showed little change in size. When $C_{AN}$ was 0.58 ($c_{AN} = 0.82$), the particles were somewhat distorted as shown in Figure 1B. The particles with a $C_{AN}$ of 0.63 ($c_{AN} = 0.87$) were also distorted. The nanoparticles with a $C_{AN}$ of 0.66 ($c_{AN} = 0.92$) were far from uniform as shown in Figure 1C. When $C_{AN}$ was 1.00 yielding poly(AN-*co*-PEGm), no particles could be prepared. Since PAN has some solubility in both water and ethanol, AN may be unable to form the stable core of the core−corona type of nanospheres, different from the case of St. In other

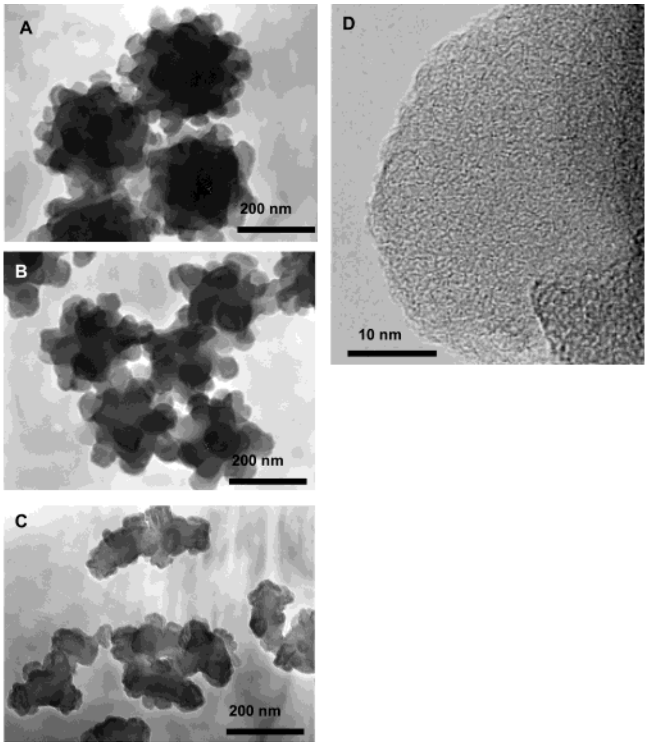

**Figure 1.** TEM images of nanoparticles of poly(styrene-*co*-acrylonitrile-*co*-PEG macromonomer)s: (A) acrylonitrile composition = 0.49; (B) acrylonitrile composition = 0.55; (C) acrylonitrile composition = 0.66; (D) expended image of projection portion of (A).

**Scheme 1. Molecular Structure of Poly(styrene-*co*-acrylonitrile-*co*-PEG macromonomer)**

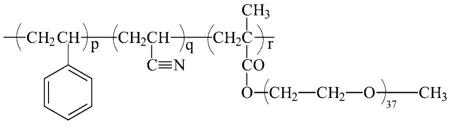

**Table 2. Synthesis and Characterization of Poly(St-*co*-AN-*co*-PEGm) for Various Polymerization Times**[a]

| polymerization time (h) | comp in terpolymer[b] St: AN | N/C[c] | O/C[c] | yield (wt %) |
|---|---|---|---|---|
| 1 | 0.47:0.53 | 0.12 | 0.29 | 29 |
| 2 | 0.44:0.56 | 0.10 | 0.41 | 33 |
| 3 | 0.44:0.55 | 0.11 | 0.48 | 44 |
| 4 | 0.44:0.56 | 0.11 | 0.51 | 46 |
| 5 | 0.45:0.55 | 0.13 | 0.54 | 49 |
| 6 | 0.44:0.55 | 0.11 | 0.53 | 52 |
| 12 | 0.43:0.56 | 0.13 | 0.60 | 56 |
| 24 | 0.44:0.55 | 0.13 | 0.62 | 48 |

[a] St, AN, and PEGm refer to styrene, acrylonitrile, and poly(ethylene glycol) monomethacrylate, respectively. The St, AN, and PEGm compositions in the feed were 23, 76, and 0.7, respectively; temperature was 60 °C; solvent was a mixture of water and ethanol (water/ethanol = 1v/4v); $M_n$ of PEGm is 1740. [b] Determined by $^1$H NMR spectra. [c] N/C and O/C refer to the molar ratio of nitrogen to carbon and that of oxygen to carbon, respectively, which were determined by ESCA.

words, St is one of the most effective monomers on nanosphere formation and forms the spherical substance required for projection formation in the nanospheres. As a consequence, AN and St cooperatively contribute to the formation of nanospheres with projection coronas.

ESCA of the nanospheres with a $C_{AN}$ of 0.49 showed distinct peaks assigned to the bonds of nitrogen and oxygen as well as carbon bonds (Figure 2), indicating the presence of AN and PEGm units on the surface. As shown in Table 1, the ratio of the integral value of the nitrogen peak to that of the carbon peak (seventh column) slightly increased with increasing $C_{AN}$ in bulk shown in the sixth column, while the ratio of the integral value of the oxygen peak to that of the carbon peak (eighth column) remained at 0.50−0.69 regardless of $C_{AN}$ in bulk. The increase in AN surface composition should be related to the increased abundance of the surface area of the projections. The independence of PEGm surface composition on bulk composition suggests that the PEG chain grafts over the particles regardless of the morphology.

The structure of the nanospheres with projections was investigated by the wide-angle X-ray diffraction (WAXD) method. Figure 3 shows the WAXD pattern of the nanospheres with $C_{AN}$ values of 0.49, 0.58, and 0.66. In the nanospheres with a $C_{AN}$ of 0.66, a distinct peak appeared at $2\theta = 17.1°$ ($\theta$: diffraction angle) corresponding to a spacing of 0.52 nm, and a large halo appeared at around $2\theta = 23°$ (Figure 3C). The peak at $2\theta = 17.1°$ can be assigned to crystals of the AN-rich segment since PAN also shows crystalline peak at $2\theta = 17.1°$ according to the literature.[22] (PEG shows crystalline peaks at other diffraction angles of $2\theta = 19.7°$ and 23.9°.[23]) The WAXD patterns of the nanospheres with $C_{AN}$ of 0.63 showed the same crystalline peak. It can be thought that the large halo around $2\theta = 23°$ is derived from an amorphous moiety. The diffraction of the PAN crystal was small in the nanospheres with $C_{AN} = 0.58$ and was undetectable in the $C_{AN} = 0.49$ nanospheres. $C_{AN}$ values where the AN-rich chains were crystallized corresponded with the value where the nanoparticle distortion was observed, suggesting the strong correlation between the distortion and AN crystallization. The St-rich chain prepared at the beginning of polymerization can form the nanosphere core where the monomers are subsequently incorporated and polymerized as confirmed in the previous paper.[24] The higher solvent affinity of AN and PEGm than St can induce the segregation of AN and PEGm domains to form a shell during polymerization. We further investigate the relationship between the projection and the AN crystal by TEM. The TEM image showed the amorphous contrast in the projection portion as shown in Figure 1D. Thus, the projection formation may not be induced by the crystal growth.

**Effects of Reaction Time.** The morphology of the projection surface is sometimes given by the dynamic factor in a nonequilibrium system.[25,26] The effects of the reaction time on the nanosphere morphology were analyzed by TEM (Figure 4) in nanospheres prepared under the reaction conditions shown in run 4 of Table 1. Yields were also low (29−56%), and $M_n$ and $M_w$ were in the ranges $2.4 \times 10^4 - 6.4 \times 10^4$ and $1.4 \times 10^5 - 1.8 \times 10^5$, respectively, which did not show a large dependence on reaction time. $M_w/M_n$ values were also widely distributed (2.7−5.7). As shown in Table 2, the AN composition did not depend on the reaction time. Since yields were almost constant after 3 h, the polymerization was practically completed in 2−3 h. However, projection growth started from 2 h as shown in the TEM images (Figure 4). Polymerization for 1 h gives the nanospheres, but no projections were formed (Figure 4A). Projections began to appear at 2 h, although they were tiny (Figure 4B). After 3 h, the TEM image of

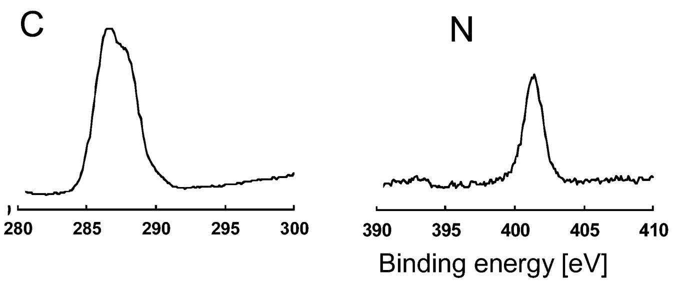

**Figure 2.** ESCA diagram in the region of carbon, nitrogen, and oxygen elements of nanoparticles of poly(styrene-*co*-acrylonitrile-*co*-PEG macromonomer)s with an acrylonitrile composition of 0.49.

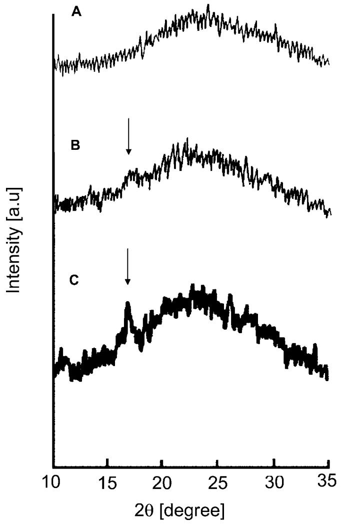

**Figure 3.** Wide-angle X-ray diffraction diagrams of poly(styrene-*co*-acrylonitrile-*co*-PEG macromonomer)s with acrylonitrile compositions of 0.49 (A), 0.58 (B), and 0.66 (C).

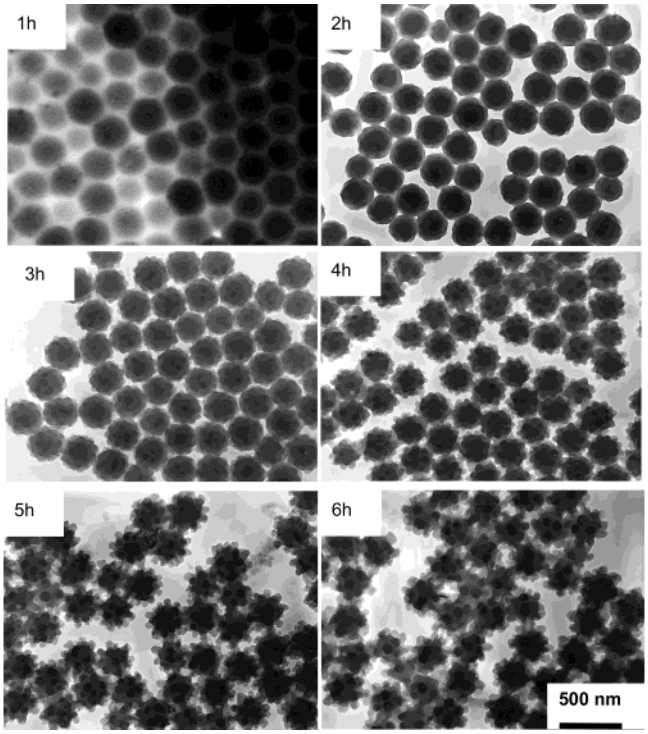

**Figure 4.** TEM images of nanoparticles of poly(styrene-*co*-acrylonitrile-*co*-PEG macromonomer)s prepared for various reaction times.

Figure 4C showed projection growth; one can see the regular arrangement of the projection on the surface, and the projections grew further after that. Figure 5A shows the time dependence of projection volume which was calculated assuming that the projections have the morphology of an elliptical hemisphere. Projections growth increased with reaction time. However, TEM images demonstrated that the number of projections per a nanosphere remained at 26 ± 2 regardless of the reaction time. Figure 5B shows the time dependence of the averaged sharpness which was estimated as the ratio of projections height to the value of full width at half-height. The sharpness increased with increasing reaction time and saturated to a certain value at about 12 h. After 12 h, the projections continue to grow while maintaining the same sharpness. From these results we can conclude that the nucleation of projection occurred almost simultaneously in less than 2 h, but after the polymerization was finished, and that the projections uniformly grew from a nucleus position preferentially toward the vertical direction of the nanosphere surface.

Figure 6 shows that relationship between the elemental composition of the nanosphere surface and the reaction time. ESCA of the nanospheres without projections prepared by polymerization for 1 h shows the distinct nitrogen peak and oxygen peak, indicating the presence of AN and PEGm units on the surface. In the course from 1 to 24 h, the ratio of nitrogen peak area to that of carbon peak area (third column of Table 2) does not show a remarkable change. This result indicated that projection growth on the surface is not directly attributable to AN surface composition. On the other hand, the ratio of oxygen peak area to that of carbon peak area (fourth column of Table 2) shows a large increase, indicating that the PEG graft chain may affect the projection formation to some extent.

SEM images confirmed that the projections covered the nanosphere surface. Especially, the nanospheres with a $c_{\mathrm{AN}}$ of 0.66 prepared by the polymerization for 3 h showed a high uniformity of the projection arranging with hexagonal symmetry like coronavirus[21] (Figure 7). On the particles 26 ± 2 projections were located at even intervals of 80 nm. If the base of the projections is assumed to be circular, the diameter and total area of the base can be estimated as about 50 nm and $5.1 \times 10^4$ nm$^2$, respectively. Since the height of the projections was measured to be 25 nm, the projection can be roughly regarded as hemispheric in morphology. On the basis of this assumption, the total surface area of the projections can be estimated as $1.0 \times 10^5$ nm$^2$, which corresponds to 25 ± 5% of the whole surface area of the nanospheres with projections ($3.1 \times 10^5$ nm$^2$). Some of the particles with a $c_{\mathrm{AN}}$ of 0.71 and 0.76 also showed the morphology like that of the coronavirus. The number of projections decreased from 26 ± 2 for $c_{\mathrm{AN}} = 0.66$ to 10 ± 3 for $c_{\mathrm{AN}} = 0.87$ with a decrease the nanosphere size. However, the abundance of the projection in terms

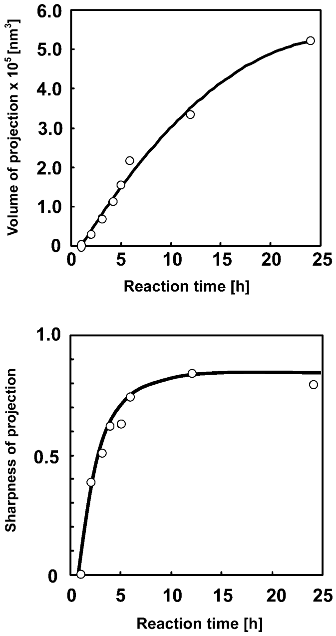

**Figure 5.** Changes in the projection volume and sharpness as a function of reaction time in the nanospheres of poly(styrene-*co*-acrylonitrile-*co*-PEG macromonomer)s.

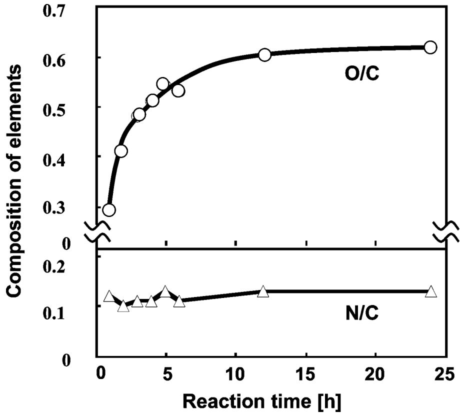

**Figure 6.** Reaction time dependence of the surface composition of nanospheres composed of poly(styrene-*co*-acrylonitrile-*co*-PEG macromonomer)s as measured by ESCA.

of the surface area gradually increased up to 85 ± 10% with increasing $c_{\mathrm{AN}}$ up to 0.87, suggesting the projections mainly correspond to AN units.

**Mechanism of Projection Formation.** A tentative mechanism of the formation of the nanoparticles with projection coronas is shown in Figure 8. At the beginning of the polymerization, the St-rich polymers form the nanosphere core where the monomers were subsequently incorporated and polymeric chains were propagated, similar to the mechanism of conventional dispersion polymerization.[27] AN and PEGm may subsequently cover the core to form the shell since they have high solvent affinity in water/ethanol solvent. The surface layer may then stabilize the water dispersion of the nanoparticles, as previously reported in the poly(St-*co*-PEGm) system.[24] In 1 h, the particles had no projection. Beyond 2 h, the amount of PEGm chains on the surface was increased with reaction time and accompanied by growth of the projections. It is widely known that the gels show a regular patterning during swelling[26] although the detail mechanism has never been clarified. In the present case, since the shell domain was backed with the solvatophobic core and capable of solvating, it can be swollen like the polymer gels. Since the swelling of the shell domain should make the chain mobility increase, the PEG chain having the free chain end can transfer from the shell domain to the surface as confirmed in the ESCA study. The PEG graft chain with the high solvent affinity could accelerate the swelling to give the projections. As a result, the projections can swell more rapidly than the portion just around the projections, which apparently yields the repulsion among the projections. Since the shell surrounded the whole area of the particle surface, this repulsive behavior must induce the regular arrangement of projections and sometimes the hexagonal symmetry on the spherical surface. The projection coronas were maintained in pure water but did not re-form in dispersions prepared from the drops of tetrahydrofuran solution of terpolymers into pure water. This result indicates that the formation of nanoparticles with projection coronas occurred simultaneously with the polymerization, and the reactivity of monomers and the

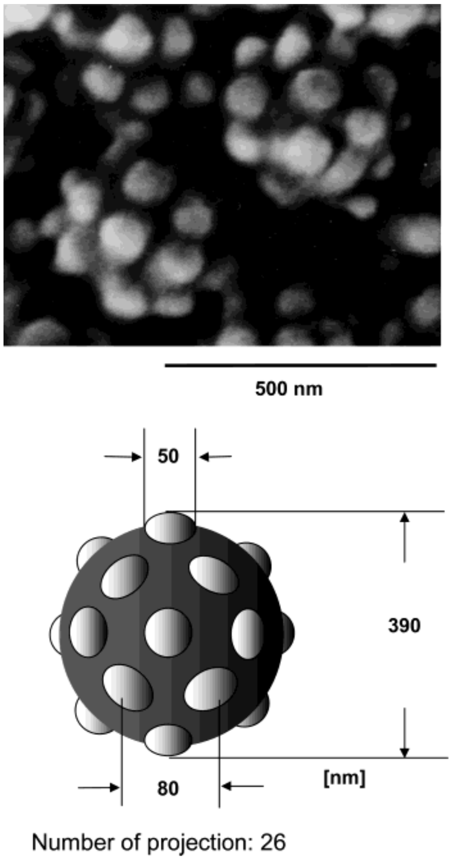

**Figure 7.** SEM image of nanoparticles of poly(styrene-*co*-acrylonitrile-*co*-PEG macromonomer) with an acrylonitrile composition of 0.49.

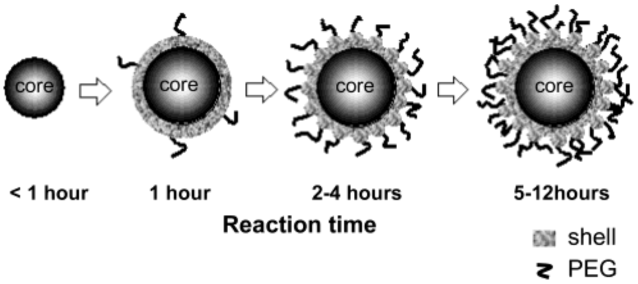

**Figure 8.** Schematic illustration of the formation mechanism of the nanoparticles with projection coronas composed of poly(styrene-*co*-acrylonitrile-*co*-PEG macromonomer)s.

solvent affinity of the polymer chains were very crucial to projection formation.

## Conclusion

Nanoparticles with projection coronas were prepared by the one-step dispersion terpolymerization of St, AN, and PEG monomethacrylate in ethanol−water solution. The morphology of the nanospheres could be controlled by changing the reaction time and terpolymer composition. When the mole composition of AN to the total monomers $C_{AN}$ was 0.49−0.66, TEM showed that the nanoparticles were spherical and had a number of projections on the surface. The nanoparticles prepared by polymerization for 3 h and under $C_{AN} = 0.49$ yielded a regular arrangement of uniform projections on the surface similar to that seen in some corona virus. The resulting nanospheres with projections had a larger specific surface area than typical nanospheres with the same diameter. It is expected that the nanospheres with projection coronas would have excellent absorption behavior similar to that of virus infection. Heteroaggregation of different particles is known to beautiful virus-like morphology.[11,12] On the other hand, the virally shaped nanospheres prepared in the present study are analogous to natural virus particles[17] in terms of the one-step formation through self-organization of the polymerizing chains.

**Acknowledgment.** This research was partly supported by a Grant-in-Aid for Tokuyama Science Foundation. We show appreciation to Mr. Kakoi, a technician of Kagoshima University, and Dr. Okunishi of JEOL for TEM studies and Mr. Ohzono, a technician of Kagoshima University, for ESCA studies.

## References and Notes

(1) Akagi, T.; Kawamura, M.; Ueno, M.; Hiraishi, K.; Adachi, M.; Serizawa, T.; Akashi, M.; Baba, M. *J. Med. Virol.* **2003**, *69*, 163.
(2) Rihova, B. *Adv. Drug Delivery Rev.* **2002**, *54*, 653.
(3) Hayward, R. C.; Saville, D. A.; Aksay, I. A. *Nature (London)* **2000**, *404*, 56.
(4) Okubo, T. *Prog. Polym. Sci.* **1993**, *18*, 481.
(5) Kitano, M.; Hamabe, T.; Maeda, S.; Okabe, T. *J. Cryst. Growth* **1990**, *102*, 965.
(6) Sun, Y.; Xia, Y. *Science* **2002**, *298*, 2176.
(7) Skjetorp, A. T.; Ugelstad, J.; Ellingsen, T. *J. Colloid Interface Sci.* **1986**, *113*, 577.
(8) Okubo, M.; Katsuta, Y.; Matsumoto, T. *J. Polym. Sci., Polym. Lett. Ed.* **1982**, *20*, 45.
(9) Okubo, M.; Yamashita, T.; Minami, H.; Konishi, Y. *Colloid Polym. Sci.* **1998**, *276*, 887.
(10) Reculusa, S.; Poncet-Legrand, C.; Ravaine, S.; Mingotaud, C.; Duguet, E.; Bourgeat-Lami, E. *Chem. Mater.* **2002**, *14*, 2354.
(11) Dubois, M.; Demé, B.; Thaddée, G.-K.; Dedieu, J.-C.; Vautrin, C.; Désert, S.; Perez, E.; Zemb, T. *Nature (London)* **2001**, *411*, 672.
(12) Hubert, H.; Devouard, B.; Garvie, L. A. J.; O'Keeffe, M.; Buseck, P. R.; Petuskey, W. T.; McMillan, P. F. *Nature (London)* **1998**, *391*, 376.
(13) Konishi, Y.; Okubo. M.; Minami, H. *Colloid Polym. Sci.* **2003**, *281*, 123.
(14) Yi, G.-P.; Moon, J. H.; Manoharan, V. N.; Pine, D. J.; Yang, S.-M. *J. Am. Chem. Soc.* **2002**, *124*, 13354.
(15) Akashi, M.; Kirikihira, I.; Miyauchi, N. *Angew. Makromol. Chem.* **1985**, *132*, 81.
(16) Chen, M.-Q. Kaneko, T.; Chen, C.-H.; Akashi, M. *Chem. Lett.* **2001**, 1306.
(17) Branden, C.; Tooze, J. *Introduction to Protein Structure*, 2nd ed.; Taylor & Francis: New York, 1999.
(18) Serizawa, T.; Takehara, S.; Akashi, M. *Macromolecules* **2000**, *33*, 1759.
(19) Boundy-Boyer *Styrene*; Reinhold Publishing Corp.: New York, 1952.
(20) Mayo, F. R.; Lewis, F. M. *J. Am. Chem. Soc.* **1944**, *66*, 1594.
(21) Matthews, R. E. F., Ed.; *Classification and Nomenclature of Viruses. Fourth Report of the International Committee on Taxonomy of Viruses;* S. Karger AG: Basel, 1982.
(22) Minagawa, M.; Taira, T.; Yabuta, Y.; Nozaki, K.; Yoshii, F. *Macromolecules* **2001**, *34*, 3679.
(23) Rajendran, S.; Mahalingam, T.; Kannan, R. *Solid State Ionics* **2000**, *143*, 130.
(24) Akashi, M.; Yanagi, T.; Yashima, E.; Miyauchi, N. *J. Polym. Sci., Polym. Chem. Ed.* **1989**, *27*, 3521.
(25) Mullins, W. W.; Sekerka, R. F. *J. Appl. Phys.* **1963**, *34*, 323.
(26) Matsuo, E. S.; Tanaka, T. *Nature (London)* **1992**, *358*, 482.
(27) Barret, K. E. J.; Thompson, M. W. *Dispersion Polymerization in Organic Media;* Barret, K. E. J., Ed.; Wiley: London, 1975.

MA035276G